Journal of Applied Polymer Science

Mechanical, Thermal, and Barrier Properties of Nanocomposites based on Poly(butylene succinate)/Thermoplastic Starch Blends Containing Different Types of Clay

Piangruetai Boonprasith,[1] Jatuphorn Wootthikanokkhan,[1] Nonsee Nimitsiriwat[2]

[1]School of Energy, Environment and Materials, King Mongkut's University of Technology Thonburi, Bangkok 10140, Thailand
[2]Pilot Plant Development and Training Institute, King Mongkut's University of Technology Thonburi, Bangkok 10140, Thailand
Correspondence to: J. Wootthikanokkhan (E-mail: Jatuphorn.woo@kmutt.ac.th)

ABSTRACT: Nanocomposites based on blends of poly(butylene succinate) (PBS) and thermoplastic cassava starch (TPS) were prepared using a two-roll mill and compression molding, respectively. Two different types of clay, namely sodium montmorillonite (CloisiteNa) and the organo-modified MMT (Cloisite30B) were used. The morphological and mechanical properties of the nanocomposite materials were determined by using XRD technique and a tensile test, respectively. Thermal properties of the composite were also examined by dynamic mechanical thermal analysis and thermal gravimetric techniques. Barrier properties of the nanocomposites were determined using oxygen transmission rate (OTR) and water vapor transmission rate (WVTR) tests. From the results, it was found that by adding 5 pph of the clay, the tensile modulus and the thermal properties of the blend containing high TPS (75 wt %) changed significantly. The effects were also dependent on the type of clay used. The use of Cloisite30B led to a nanocomposite with a higher tensile modulus value, whereas the use of CloisiteNa slightly enhanced the thermal stability of the material. OTR and WVTR values of the blend composites containing high PBS ratio (75 wt %) also decreased when compared to those of the neat PBS/TPS blend. XRD patterns of the nanocomposites suggested some intercalation and exfoliation of the clays in the polymer matrix. The above effects are discussed in the light of different interaction between clays and the polymers. © 2013 Wiley Periodicals, Inc. J. Appl. Polym. Sci. 000: 000–000, 2013

KEYWORDS: composites; clay; blends; Biopolymers and renewable polymers

Received 8 October 2012; accepted 14 March 2013; Published online 00 Month 2013
DOI: 10.1002/app.39281

INTRODUCTION

The use of biodegradable plastics as alternative materials for various applications has gained more and more interest over the past decade. This is driven by the fact that many bioplastics, such as are environmentally friendly and biodegradable. These include polylactide (PLA) polycaprolactone (PCL), poly(butylene succinate) (PBS) and thermoplastic starch. Among the above-mentioned bioplastics, PBS, which is chemically synthesized by polycondensation of butanediol and succinic acid, has many useful properties including a high heat distortion temperature, melt processability, high toughness and biodegradability. However, the price of PBS resins is still high compared to those of many commodity plastics.[1] To promote more commercial use of the polymer, the material cost should be decreased. This can be achieved by blending PBS with other natural polymers such as thermoplastic starch (TPS). In this regard, compatibility between PBS and TPS is an important factor, affecting the mechanical and barrier properties of the product. However, the above problem can be solved by using appropriate compatibilizers[2–4] and/or chemically modifying polymers prior to blending in order to promote a stronger molecular interaction.[5–7]

Furthermore, for some applications such as food packaging, the gas barrier properties of the materials are important and should also be enhanced. This can be controlled by various strategies including the use of multilayer films and/or by mixing polymers with nanoclay. In the latter case, a decrease in the oxygen transmission rate (OTR) and water vapor transmission rate (WVTR) of many polymer nanocomposites has been reported.[8] The results were ascribed to a tortuous path, provided by the exfoliation structure of the nanocomposite. In this regard, the microstructures and properties of the nanocomposites depend on interaction between the polymer and the nanoclay, which is in turn governed by the chemical structure and composition of the composite materials.

For example, Ray et al.[9] demonstrated that the solubility parameter of Cloisite30B is close to that of PBS. Consequently,

an intercalation structure of PBS/Cloisite30B composite system was observed.[9,10] This effect is attributed to a strong interaction between hydroxyl groups in the gallery of Cloisite30B and the carboxylic groups of PBS. Similar results were also observed in the PLA/Cloiste30B nanocomposite system.[11] This was not the case, however, for the PLA nanocomposite containing CloisiteNa. This is due to the fact that CloisiteNa lacks hydroxyl groups for reacting with the functional groups of PLA molecules. However, CloisiteNa seems to be more compatible with some hydrophilic polymers such as starches. Park et al.,[12,13] for example, found that the use of CloisiteNa led to intercalation of thermoplastic starch in the gallery of the silicate later. As a result, both the tensile properties and resistance to water vapor transmission of the materials were improved. The above results are discussed in the light of polar interaction between the hydroxyl groups of TPS and the silicate layer of the inorganic CloisiteNa. Lee et al.[14] studied the microstructure of aliphatic polyester/organoclay nanocomposites and found that the degree of intercalation in polyester/Cloisite30B hybrid systems is greater than that of the polyester/Cloisite10A systems. Again, the above effect is related to a strong interaction between the carboxylic groups of the polyester and the hydroxyl groups in the gallery of Cloisite30B.

Notably, Bocchini et al.[10] prepared thermoplastic starch (TPS) nanocomposites and found that melt blending of TPS with either CloisiteNa or Cloisite30B did not lead to exfoliation or intercalation of starch chains into the clay layers. In our opinion, any discrepancy could be attributed to differences in the clay loading and melt viscosity of the composite material during mixing. Interestingly, by blending the TPS/nanoclay with 20 wt % of poly(butylene succinate-*co*-adipate) (PBAS), exfoliation of polymer chains into the Cloisite30B gallery was observed.[10] In that case, the results were ascribed to a high affinity between Cloisite30B and PBAS. However, the effects of PBSA/TPS blend ratio on the microstructure and properties of the polymer nanocomposites were not reported.

From the above literature review, it seems that the microstructure and resulting properties of polymer nanocomposites depend on many factors including the type and content of the nanoclay used as well as the chemical structure and hydrophilicity of the polymer matrix. Furthermore, in relation to nanocomposites comprising immiscible polymer blends, a suitable type of clay can be different from that for the relevant homopolymer composite systems. Besides this, the effects of blend composition on the microstructure of polymer nanocomposite are still unclear. This is an aspect deserving further investigation. In this study, nanocomposites based on blends of poly(butylenes succinate) (PBS) and thermoplastic starch (TPS), compatibilized with maleic anhydride grafted poly(butylene succinate) (PBS-*g*-MA), are of interest. Two types of commercially available clay, namely CloisiteNa and Cloisite30B, having different polarity were used for developing the PBS/TPS blend nanocomposites. The aim of the study is to investigate the effects of clays and the use of the compatibilizer on mechanical, thermal, and barrier properties of various PBS/TPS blends.

EXPERIMENTAL

Chemicals

The starch used in this study was a cassava starch, supplied by E.C.T. International Co. (Bangkok, Thailand). It contained 17% amylose and 79% amylopectin, with minor amounts of lipids, proteins, and phosphorus. Glycerol (commercial grade), used as a plasticizer for the starch, was supplied from Lab System Co. (Bangkok, Thailand). Poly(butylenes succinate) (PBS) (AZ-91TN; food grade product), used for preparing the PBS/TPS blends, was purchased from Mitsubishi Chemical Corporation (Tokyo, Japan). Dicumyl peroxide (DCP; 98%) and maleic anhydride (MA; 98%) were purchased from Sigma-Aldrich and Fluka, respectively, and were used as received. Sodium montmorillonite (CloisiteNa) and organo-montmorillonite modified clay with methyl, hydrogenated tallow, *bis*-2-hydroxyl, quaternary ammonium, (Cloisite30B), were supplied from Southern Clay Product.

Preparation of Maleic Anhydride Grafted Poly(butylene succinate)

Maleic anhydride grafted poly(butylene succinate) (PBS-*g*-MA), to be used as a compatibilizer for this blend system, was prepared by mixing 285 g of PBS with MA (8.8 g) and DCP (2.2 g) in an internal mixer (Brabender, 350/350E), using a fill factor of 0.8. The mixing machine was operated at a rotor speed of 50 rpm, at 140°C for 5 min. After that, the product was removed from the mixer and then washed with stirred methanol for 24 h to get rid of residual unreacted MA. The purified product was dried in an oven at 80°C for 24 h. The chemical structure of the PBS-*g*-MA was confirmed by ^{1}H-NMR analysis, using a Bruker instrument (DPX300 Ultrashield, 300 MHz).

Materials Compounding and Fabrication

Thermoplastic Starch (TPS). The cassava starch was dried in an oven at 80°C for 24 h prior to compounding. After that, 30 wt % of glycerol was mixed with the dried starch in an internal mixer (Brabender 350/350E), using a fill factor of 0.66. The mixing was carried out at 60 rpm, 110°C, for 25 min.

PBS/TPS Nanocomposites. The dried PBS was fed into a two-roll mill (Chaichareon Karnchang Co.) at 140°C, followed by adding TPS, and clay (5 pph). To improve the compatibility between the PBS and TPS, 5 pph of PBS-*g*-MA was also added to the blend compound. Notably, according to the literature,[15–17] the optimum content of MA grafted polymers for use as a compatibilizer in many aliphatic polyester blends and composites ranges between 3 and 10 pph. In this study, 5 pph of PBS-*g*-MA was used. The mixing was carried out for 10 min, using different PBS/TPS weight ratios (25/75, 50/50, and 75/25% w/w). After that, the mixture was pelletized and dried at 70°C for 2 h in a vacuum oven. With the absence of PBS-*g*-MA, similar procedures were used to prepare the normal PBS/TPS nanocomposites.

The pelletized composite was then fabricated into 15×15 cm^2 rectangular test pieces, using a hydraulic compression molding machine (Chareontut Co., PR1D-W300L300HD), equipped with a 0.5 mm thick mold. The sample was pre-heated at 140°C for 7 min before molding. The molding was conducted under a pressure of 100 bar for 2 min and 150 bar for 3 min,

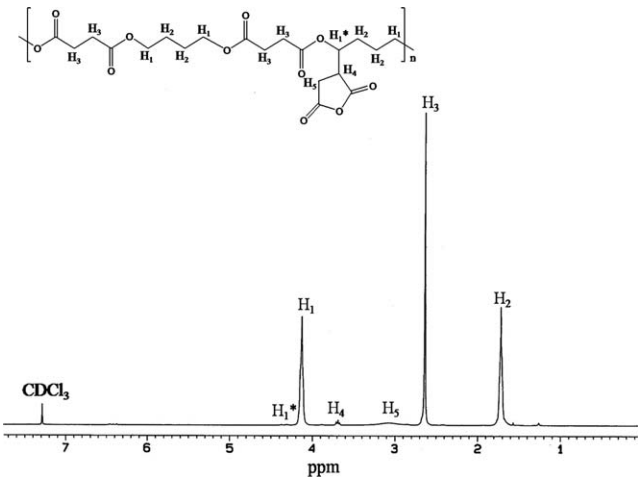

Figure 1. [1] H-NMR spectrum for the PBS-*g*-MA in $CDCl_3$.

respectively. After that, the fabricated sample was cooled to 40°C in the mold for 5 min before removal.

Characterizations

Microstructure and Morphology. The morphology of the various blends was examined by using a scanning electron microscopy (SEM) technique. The SEM specimens were prepared by cryogenic fracturing of the rectangular test-pieces, at liquid nitrogen temperature. Prior to the SEM experiment, the surfaces of the specimens were coated with Au, using a gold sputtering technique (SPI-module^{TM} coater, S/N 10081) in order to avoid some charging effect during the electron beam scanning. The SEM experiment was operated using a JEOL (JSM5800) machine (Tokyo, Japan), equipped with a secondary electron detector, using an accelerating voltage of 10 kV.

The intercalation and exfoliation structures of the nanocomposites were investigated using an X-ray diffraction (XRD) technique with a diffractometer (D8-Discover model from Bruker AXS). The operation was in the *y–y* geometry. The instrument used radiation from a copper target tube (Cu *Kα* radiation wavelength of 1.5406 Å). The XRD data were collected between 2 and 60 in a step size of 0.02 degree/step, with an X-ray generator.

Mechanical Properties. The mechanical properties of the various blends and nanocomposites were determined using a universal testing machine (LLOYD; LR 50K). Dumbbell-shaped specimens were prepared by cutting the sheet using a suitable die in accordance with ASTM D638. The tensile test was carried out at a crosshead speed of 100 mm/min, using the 1000 N load cell. At least five specimens were tested for each sample and the average values of Young's modulus, tensile strength at break, and elongation at break were then calculated and reported.

Thermal Properties. The thermal properties of various PBS/TPS compounds were determined using a dynamic mechanical analyzer (GABO, EPLEXOR QC25 model) in accordance with ASTM D623. The dynamic mechanical thermal analysis (DMTA) experiment was operated under a tension mode, at 1% static strain, 0.05% dynamic strain, 2 N, 1 Hz oscillating frequency, and 10 m amplitude. The heating rate used was 3°C/min and the sample was scanned over temperatures ranging between −80 and 100°C. The thermal stability of the polymer composites was also determined by thermal gravimetric analysis (TGA). The TGA experiment was carried out with a Mettler Toledo instrument (TGA/DSC1HT/1600/673/13558 model). About 5 mg of the sample was used and the TGA experiment was scanned over temperatures ranging between 25 and 700°C under nitrogen atmosphere, at a heating rate of 10°C/min.

Permeability Tests. The oxygen transmission rates (OTR) of the PBS/TPS nanocomposites were determined using an oxygen permeation tester (Illinois, 8000) equipped with a Coulometric Sensor. The test was carried out at 23°C, 0% RH, and in accordance with ASTM D3985-05. Water vapor transmission rates (WVTR) of the samples were determined using a water vapor permeation tester (Lyssy, L80-4000) using a humidity detection sensor. The test was conducted at 38°C and 90% RH, in accordance with ISO 15106-1: 2003 (E). Noteworthy: three fabricated sheets were prepared and tested for each of the nanocomposite samples. Furthermore, each sample sheet was randomly sampled and tested from five different areas before an average OTR and/or WVTR were reported.

RESULTS AND DISCUSSION

Figure 1 shows the ^{1}H-NMR spectrum of the PBS chemically modified by reacting with MA. Apart from the signals at 4.13, 1.72, and 2.64 ppm, which represent the protons from PBS molecules, new peaks at 3.7 ppm and 3.1 ppm emerged. These can be ascribed to the signal from methine and methylene protons of the MA ring, respectively. The signal at 4.4 ppm refers the methine proton in the PBS chain, which was shifted from 4.13 ppm, after grafting. The above results indicated that PBS-*g*-MA was successfully prepared.

Figures 2–4 show the tensile properties of the PBS/TPS blends with a variety of blending ratios. It can be seen that the Young's modulus and tensile strength of the material decreased linearly with the TPS content. This could be attributed to the fact that the thermoplastic starch was plasticized with glycerol. Consequently, the greater the starch content, the lower the tensile properties. However, percentage elongation values of the PBS/TPS blends are considerably low, regardless of the blending ratios. This can be ascribed to an incompatibility between the two polymers. PBS is relatively more hydrophobic than TPS, owing to the fact that repeating units of the latter molecules contain several hydroxyl groups. Consequently, an interfacial adhesion between phases might be insufficiently strong. This statement is supported by SEM images of the blends [Figure 5(a–c)], which show that the two polymers are phase separate, containing some voids, and/or gaps at the interface. This interface acts as a weak point and/or a kind of stress concentrator, lowering the mechanical properties of the specimens. After adding PBS-*g*-MA (5 pph) to the blends, the tensile strength, and modulus of the blend increased (Figures 2–4). SEM images of the samples [Figures 5(d–f)] also reveal that the blends became more homogeneous and the starch particles adhered better to the PBS matrix.

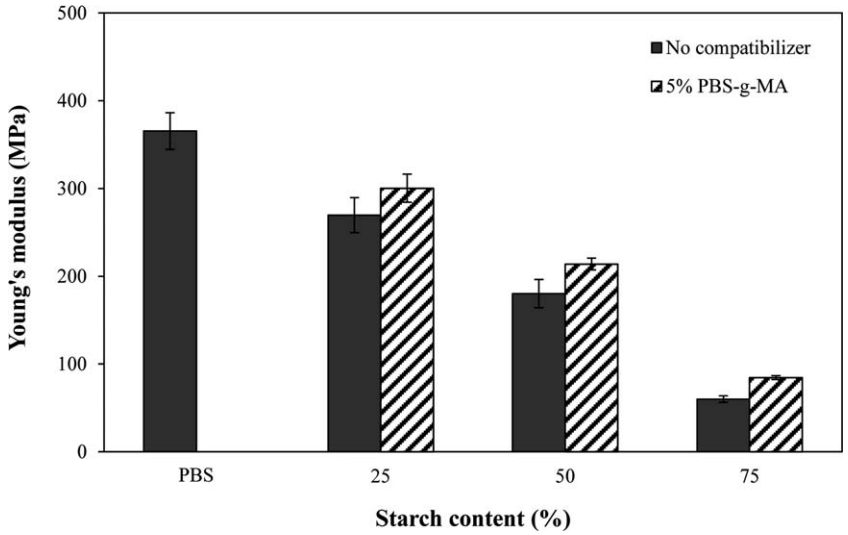

Figure 2. Tensile modulus of various PBS/TPS blends.

This indicates a good compatibilizing efficacy for the copolymer for this blend system.

Figure 6 shows DMTA thermograms of the PBS/TPS blends. The tan δ peak at around $-18^{\circ}C$, representing the glass transition temperature of the PBS, can clearly be seen from the thermogram of the blend containing a high amount of PBS (75 wt %). By increasing the TPS content in the polymer blend, a peak at $-60^{\circ}C$ can be observed and that could be ascribed to a transition temperature for the glycerol-rich TPS phase. A similar peak was also observed in the DMTA thermograms of the gelatinized starch/polyester blends, prepared by Dean et al.[18] and Park et al.[12,19] The magnitude of this peak also increased with the starch content. This was due to the fact that the higher the amount of TPS, the more the glycerol content. In addition, a broad peak over the temperatures ranging between -30 and $55^{\circ}C$ also emerged. The peak could be ascribed to a tan δ peak of an amorphous phase of TPS being overlapped with the T_g of the PBS. Similar DMTA profiles were also observed from the thermograms of the PBS/TPS blends containing the PBS-*g*-MA compatibilizer.

Figures 7–9 show the tensile properties of the various PBS/TPS nanocomposites. Notably, tensile strength and Young's modulus of the polymer blends decreased after mixing with CloisiteNa. The above effect was not the case when Cloisite30B was used. In the latter case, the tensile properties are comparable to those of the control system (without any clay). In our opinion, an inferior tensile modulus of the nanocomposite containing CloisiteNa might be attributed to the different interactions between

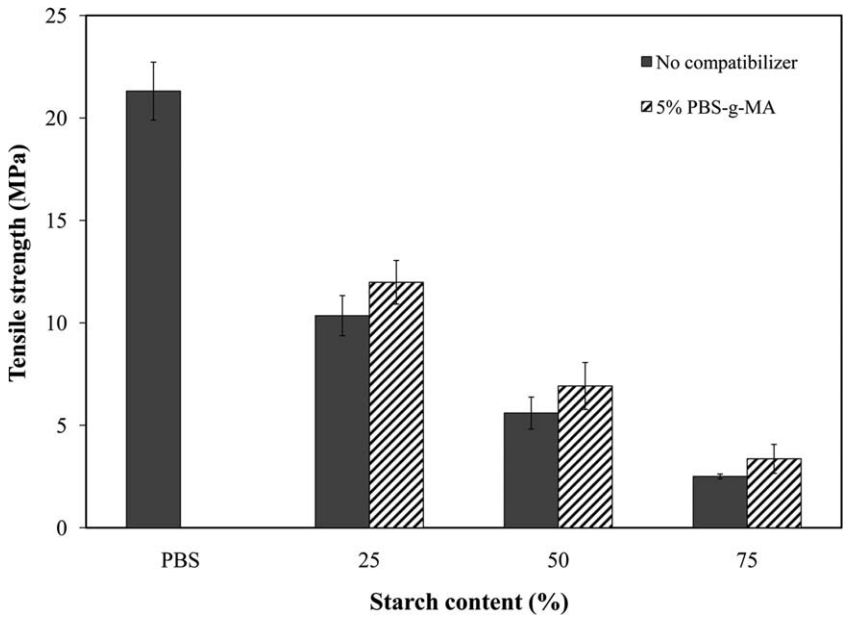

Figure 3. Tensile strength of various PBS/TPS blends.

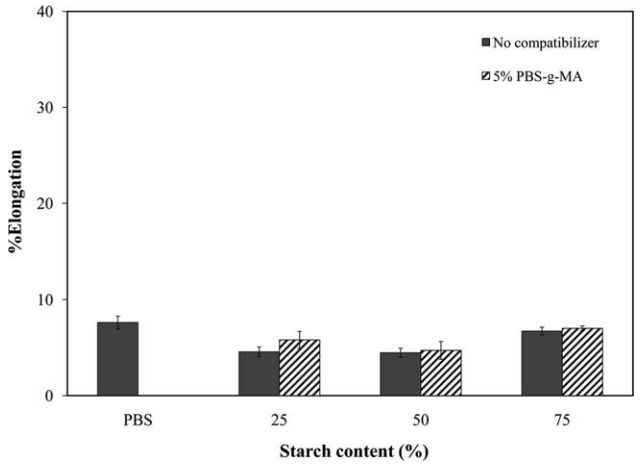

Figure 4. Elongation of various PBS/TPS blends.

the polymers and the various Cloisites. Park et al.,[19] for example, studied the mechanical properties of TPS nanocomposites containing different types of clay and found that the use of CloisiteNa led to a nanocomposite with greater tensile properties than its analogue containing Cloisite30B. The results were discussed in the light of different interaction between thermoplastic starch and the clays. In relation to this study, however, it is worth noting that the matrix phase is a PBS/TPS blend and not the TPS alone. This means that the polarity of the former matrix phase can be different from that of the latter, taking into account to the fact that PBS is less hydrophilic than TPS. In this regard, it is apparent that the polarity of CloisiteNa does not match well with that of PBS/TPS in comparison to the Cloisite30B. On the other hand, better interaction between the PBS/TPS blend and the Cloisite30B can be expected. This is attributed to a strong interaction between hydroxyl groups in the gallery of Cloisite30B and the carboxylic groups of PBS. The above notion is in good agreement with the results from the literature, demonstrating that the solubility parameter of the Cloisite30B is close to that of PBS,[9] and an intercalation structure of PBS/Cloisite30B composite system was observed.[9,10] In this study, it is of noteworthy that for the blend containing high thermoplastic starch (TPS) content (75 wt %), modulus value

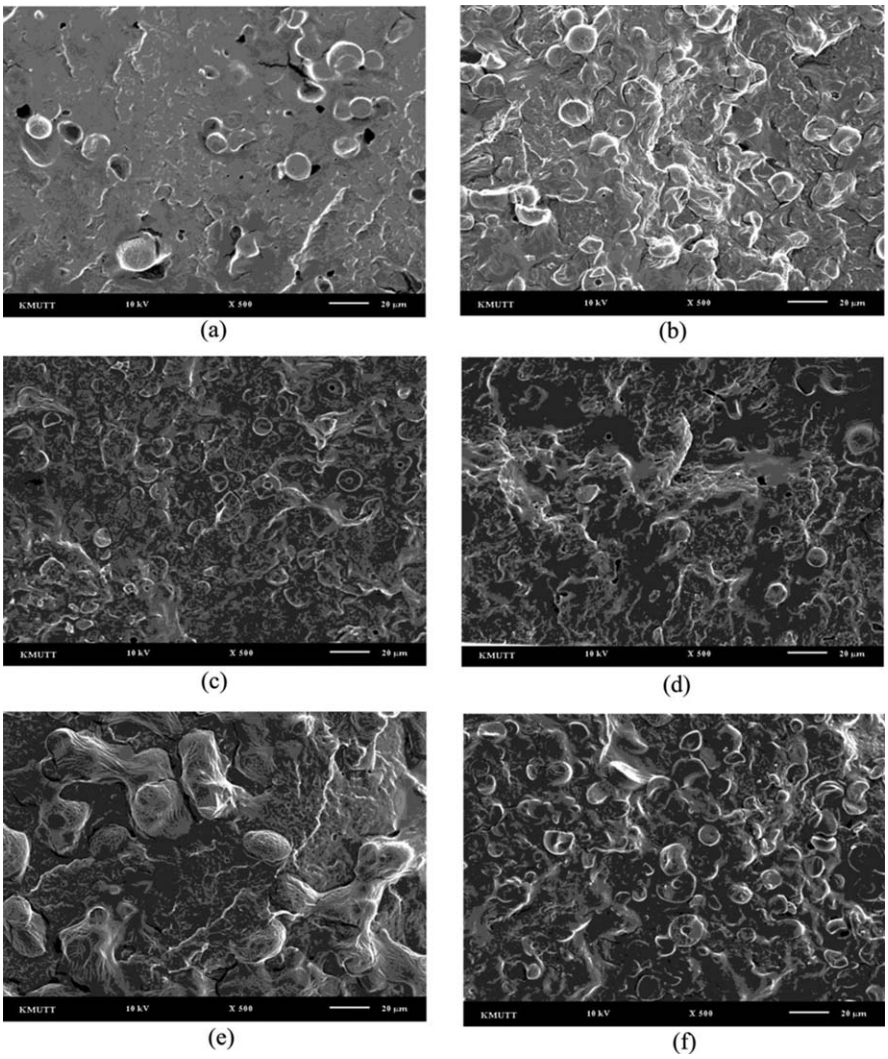

Figure 5. Scanning electron micrographs of various PBS/TPS blends; (a) PBS/TPS (75/25% w/w), (b) PBS/TPS (50/50% w/w), (c) PBS/TPS (25/75% w/w), (d) PBS/TPS (75/25% w/w) with PBS-*g*-MA, (e) PBS/TPS (50/50% w/w) with PBS-*g*-MA, and (f) PBS/TPS (25/75% w/w) with PBS-*g*-MA.

Applied Polymer SCIENCE

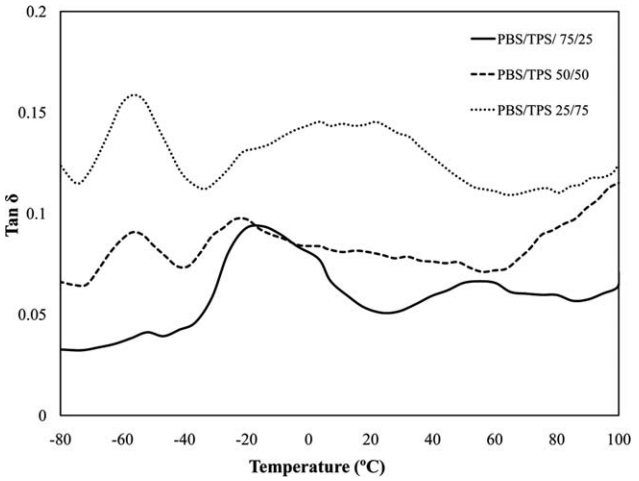

Figure 6. DMTA thermograms of PBS/TPS blends.

of the nanocomposite was significantly increased significantly after adding Cloisite30B (Figure 9). This was not the case for the nanocomposites containing lower TPS contents and the difference could be ascribed to a dilution effect and the fact that thermoplastic starch phase is inherently soft. After adding an appropriate reinforcing filler, substantial improvement of tensile modulus can be expected. Noteworthy, types of clay also play role in tensile modulus of the nanocomposite material. The use of CloisiteNa did not lead to the increase of tensile modulus of the material as was in the case of Cloisite30B. In our opinion, the above discrepancy was attributed to two main factors, i.e., the state of compatibility between Cloisites and PBS and morphology of the PBS/TPS matrix phase. According to the SEM images (Figure 5) it was noted that PBS/TPS blends are phase separated, with the TPS minor phase being dispersed within the continuous PBS phase, regardless of the blending ratios. In this regard, tensile modulus of the materials could be predominated by composition and mechanical properties of the continuous PBS matrix phase. Cloisite30B and PBS are known to be compatible. In addition, majority of the clay could have been resided within the PBS phase owing to a thermodynamic driving force. In this regard, an increase in tensile modulus of the nanocomposite can be expected. The above effect was not the case, however, when the CloisiteNa was used. In this latter case, CloisiteNa did not mix well with the PBS. Besides, some of the clay might have been preferentially resided within the TPS dispersed phase. Consequently, tensile modulus of the material was not improved significantly.

Besides this, changes in the viscoelastic properties of the PBS/TPS blend after adding the clays might also play a role. Figure 10 shows a DMTA thermogram of PBS/TPS blends (25/75% w/w) containing different types of clays. It can be seen that the magnitude of the broad tan δ peak (ranged from $-20^{\circ}C$ to $40^{\circ}C$ representing both TPS and PBS phases) decreased after mixing with the Cloisite30B. On the other hand, the tan δ_{max} of the nanocomposite system containing CloisiteNa increased when compared to that of the normal PBS/TPS blend. This suggests that the viscous component of the material increased after being mixed with the CloisiteNa. In our opinion, the result might be related to a disruption of the starch granule structure (gelatinization), owing to the presence of some moisture in the compound. Specifically, CloisiteNa is known to be more hydrophilic than the organically modified clay (Cloisite30B). Therefore, the former clay might induce a greater degree of gelatinization of the starch. The similar effect was noted from a study on PE/CloisiteNa nanocomposite system by Choi et al.[20]

Besides, the increase in the "liquid-like" behavior of PBS/TPS 25/75 could also be attributed to the intercalation of starch in the interlayer (Figure 11).

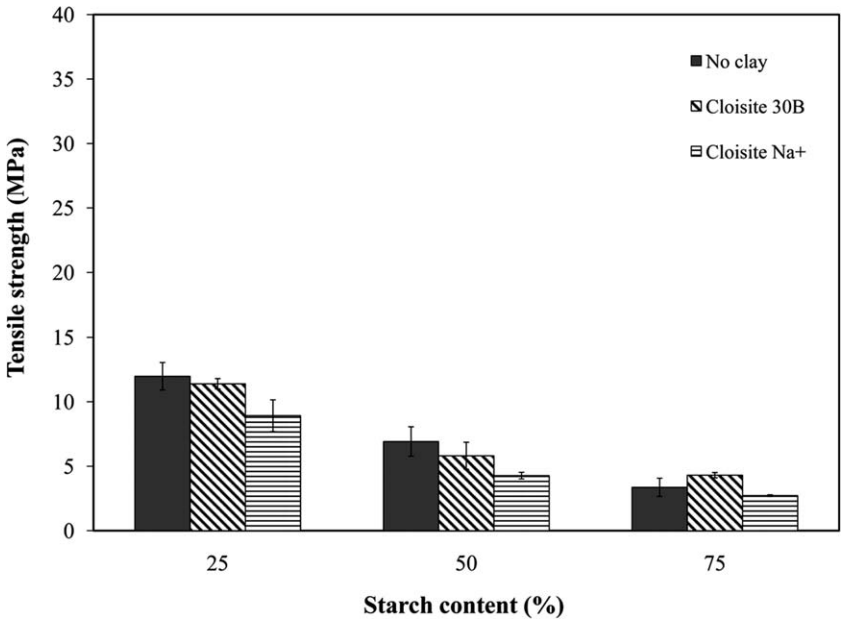

Figure 7. Tensile strength of various PBS/TPS blend nanocomposites.

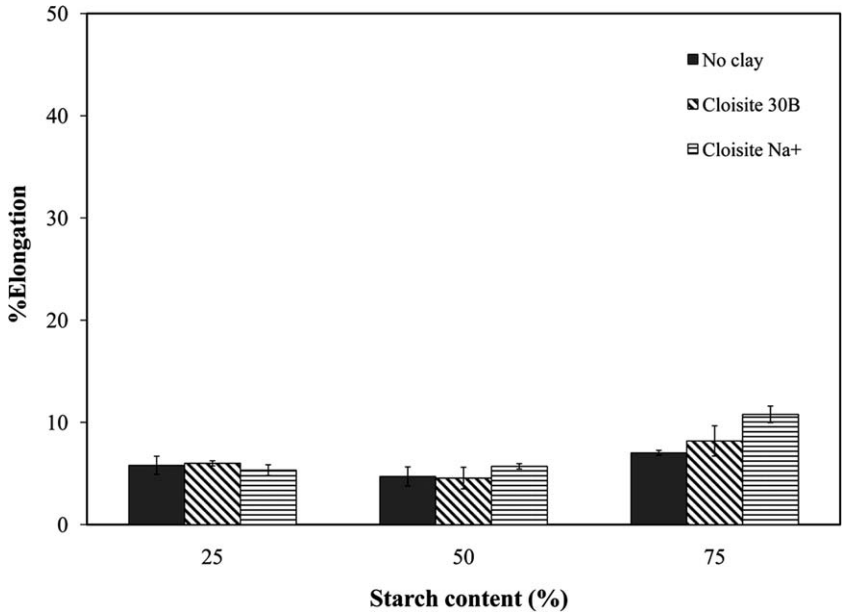

Figure 8. Elongation of various PBS/TPS nanocomposites.

XRD Results

Besides polymer–clay interactions, the microstructure of the various PBS/TPS nanocomposites also deserves consideration. Figures 11–13 show XRD patterns of CloisiteNa, Cloisite30B, and related blend nanocomposites. The peak at 7.18°, representing an interlayer distance ($d_{001} = 1.23$ nm) of the CloisiteNa[21,22] can be noted from the XRD pattern of the pure nanoclay. Similarly, the peak at 4.74° corresponding to the interlayer distance ($d_{001} = 1.86$ nm) of the Cloisite30B[10] can be seen from the XRD pattern of the clay. After mixing the PBS/TPS (25/75% w/w) blend with CloisiteNa, the peak at 7.18° shifted to the lower theta angles (4.80–5.08°; Figure 11). This suggests that the d_{001} spacing of the clay layer has been increased. Of note, our control experiment concerning the XRD pattern of the TPS/CloisiteNa nanocomposites revealed that the d_{001} spacing of the CloisiteNa also increased. A similar result was also reported by Park et al.[12] and the result was ascribed to an intercalation structure of the clay. In relation to this study, it might also be possible that the CloisiteNa has been intercalated by the thermoplastic starch phase of the blend, owing to a similar affinity.

Notably, for the same polymer matrix system containing Cloisite30B, the peak at 4.74°, corresponding to the d_{001} spacing of the Cloisite30B cannot be seen. The lack of a peak corresponding to the d_{001} spacing of Cloisite30B in the XRD pattern of the blend nanocomposite implies that some of the clay might have been exfoliated within the polymeric phase. Similar XRD patterns were observed for the nanocomposite system containing 50 wt % of thermoplastic starch (Figure 12). It would be very premature, however, to conclude that the lack of XRD peak

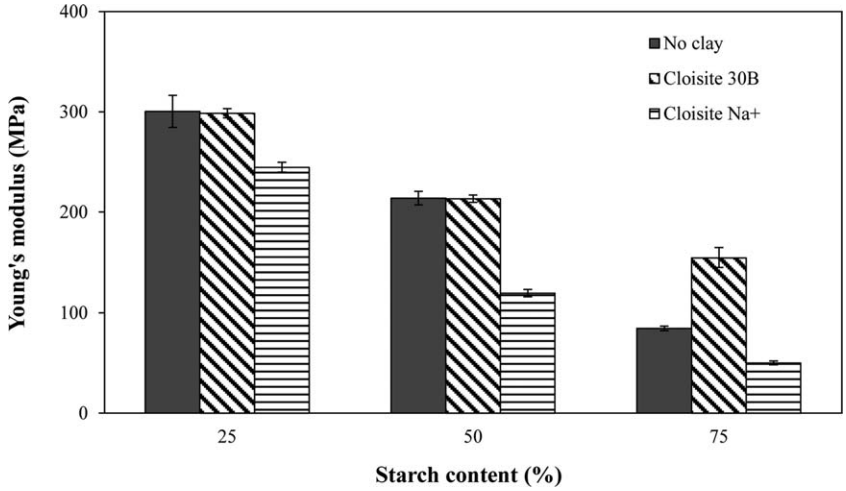

Figure 9. Modulus of various PBS/TPS nanocomposites.

Applied Polymer SCIENCE

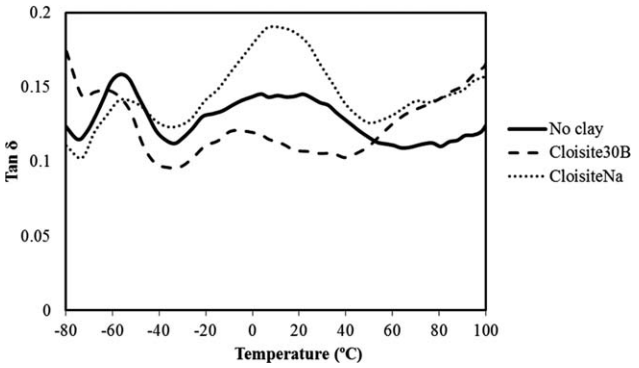

Figure 10. DMTA thermograms of PBS/TPS (25/75% w/w) nanocomposites containing different types of clay.

corresponding to d_{001} spacing of the clays indicated a complete exfoliated morphology of the nanocomposites. It might also be possible that the clays are agglomerated and phase separated from the polymer matrix phase. Consequently, if the XRD signal was generated from the matrix phase, containing no clay, then the similar XRD pattern can also be obtained. In this regard, additional information such as TEM micrographs of the nanocomposites has yet to be considered to verify the exfoliation structure.

The XRD patterns of the PBS/TPS nanocomposites containing lower TPS content (25 wt %) are quite different (Figure 13). First, the Cloisite30B peak at 7.18° shifted to the lower theta angles (3.20°). This result suggests that the d_{001} spacing of the Cloisite30B clay layer has been increased and an intercalation structure of the clay might have been created in this matrix system. Second, the peak at 7.18° belonging to the CloisiteNa disappeared. Again, additional experimental evidence from TEM technique has yet to be considered in order to confirm that some of the CloisiteNa have been exfoliated within the polymeric phase.

Thermal Stability. Figure 14 shows TGA thermograms of the neat PBS, TPS, and the PBS/TPS blend (25/75% w/w) containing different types of clay. A three-step transition can be observed from the thermogram of the blend. The first transition, occurring over temperatures ranging between 90 and 250°C, could be ascribed to dehydration and the elimination of

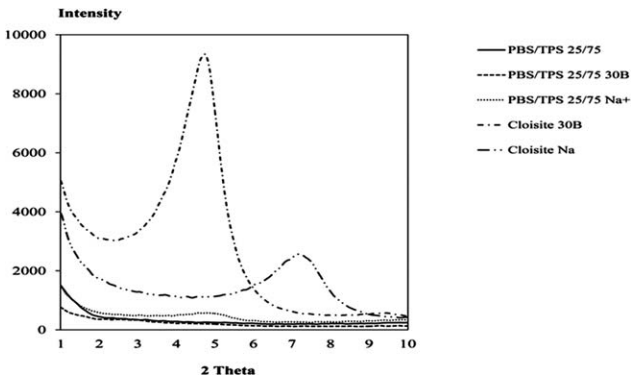

Figure 11. XRD patterns of CloisiteNa, Cloisite30B and the related PBS/TPS (25/75% w/w) nanocomposites.

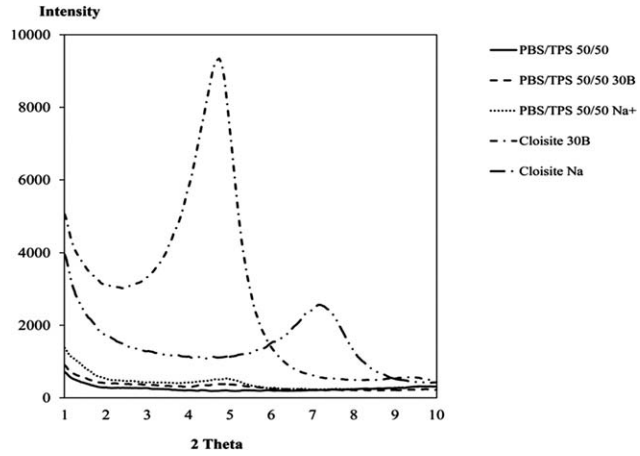

Figure 12. XRD patterns of CloisiteNa, Cloisite30B and the related PBS/TPS 50/50% w/w) nanocomposites.

glycerol in the TPS phase. Next, a sharp transition occurring over temperatures ranging between 280°C and 330°C represents the decomposition of polysaccharide and/or the TPS phase in the blend. Finally, a transition which commenced at the onset temperature of about 380°C can be attributed to the decomposition of the PBS. In this regard, the remaining weight at temperatures above 430°C could be related to some residual solid and char attributed to the TPS phase of the blend. After adding CloisiteNa to the blend, the percentage weight loss corresponding to the dehydration and elimination of glycerol decreased. The decomposition temperature of the PBS phase also shifted slightly to a higher temperature. These results suggest that the thermal stability of the PBS/TPS/CloisiteNa nanocomposite is greater than that of the normal PBS/TPS blend. A similar effect was observed by Park et al.[13] in a study on TPS/nanoclay composites. The results can be explained in the light of a strong polar interaction between CloisiteNa and the TPS phase of the blend, which promotes better interfacial adhesion and effective heat transfer between the nanoclay and the polymer matrix. Noteworthy that the above effect was not observed in TGA thermograms of the PBS/TPS/CloisiteNa nanocomposite containing lower starch content (25 wt %; Figure 15). This could be partly

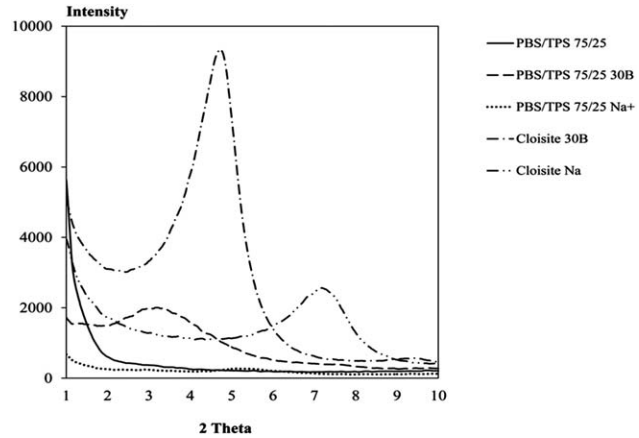

Figure 13. XRD patterns of CloisiteNa, Cloisite30B and the related PBS/TPS (75/25% w/w) nanocomposites.

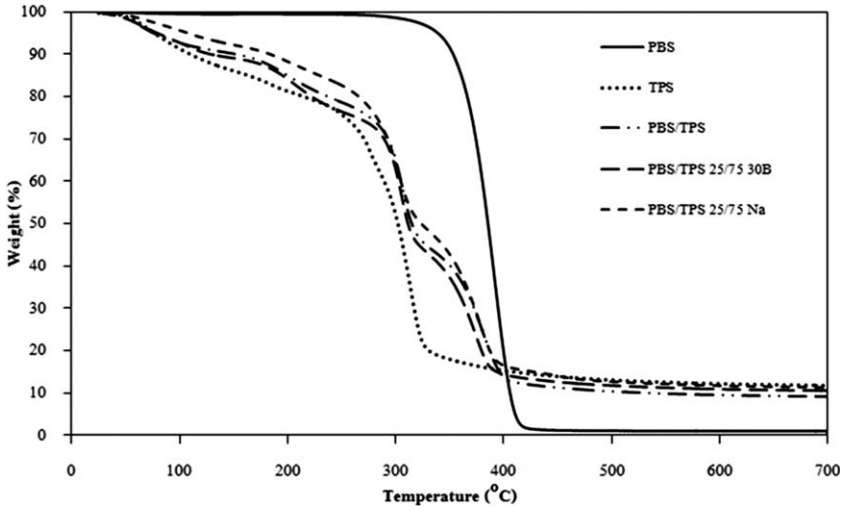

Figure 14. TGA thermograms of PBS, TPS, and PBS/TPS (25/75% w/w) nanocomposites containing different types of clay.

attributed to the fact that the starch became a minor phase and thus the effect of the CloisiteNa/TPS interaction on the thermal stability of the nanocomposite material became less dominant.

Barrier Properties. Last but not least, barrier properties of the PBS/TPS nanocomposites deserve consideration. Table I shows the oxygen transmission rates (OTR) and water vapor transmission rates (WVTR) of the PBS/TPS blend nanocomposites, containing different types of clay. It can be seen that OTR value of the polymer blend (75 wt % TPS) did not change remarkably after mixing with the clays, regardless of the clay type. Notably, there is a discrepancy between the above OTR results and their XRD patterns. The XRD results suggest that the microstructure of the nanocomposites changed with clay type. On the other hand, the averaged OTR values of the various nanocomposites are very close and not significantly different, taking into account the standard deviation values. In our opinion, this can be attributed to the fact that the OTR value of the TPS is inherently low[23] and the presence of clay in the PBS/TPS matrix cannot override the above effect. Furthermore, it was found that the WVTR values of the PBS/TPS nanocomposites could not be tested as the majority of the material contains a high amount of thermoplastic starch, which is sensitive to moisture and water vapor.

In contrast, for the blend containing low starch content (25 wt %), the use of clays significantly affected the OTR and the WVTR values of the materials. In this regard, it can be seen that both the OTR and WVTR transmission rates decreased rapidly after mixing the PBS/TPS (75/25% w/w) with the Cloisite30B. This improvement might be ascribed to the tortuous structure formed by the exfoliation and intercalation of clays as was suggested from the above XRD patterns (Figure 12). Notably, it was also found that the use of Cloisite30B is more effective than the use of CloisiteNa in terms of reducing water vapor transmission rates. In our opinion, the above discrepancy could be related to the fact that CloisiteNa is more hydrophilic than Cloisite30B.[24] Consequently, water uptake of the system

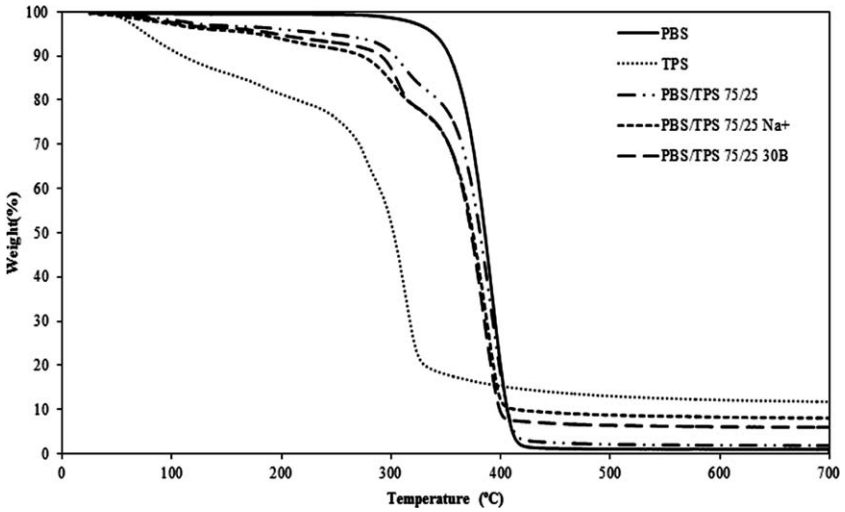

Figure 15. TGA thermograms of PBS, TPS, and PBS/TPS (75/25% w/w) nanocomposites containing different types of clay.

Table I. OTR and WVTR Values of PBS/TPS Nanocomposites Containing Different Types of Nanoclay

Samples	Clay type (5 pph)	WVTR (g m^{-2} day^{-1})	OTR (cm^3 m^{-2} day^{-1})
PBS/TPS (75/25% w/w)	None	55.4 ± 11.08	1.361 ± 136.10
PBS/TPS (75/25% w/w)	Cloisite 30B	17.7 ± 3.54	3.18 ± 0.64
PBS/TPS (75/25% w/w)	Cloisite Na^+	36.0 ± 7.20	2.40 ± 0.48
PBS/TPS (25/75% w/w)	None	n/a	5.03 ± 1.00
PBS/TPS (25/75% w/w)	Cloisite 30B	n/a	8.26 ± 1.65
PBS/TPS (25/75% w/w)	Cloisite Na+	n/a	8.94 ± 1.78

containing Cloisite30B might be less and so its WVTR can be lower.

CONCLUSION

The effects of two different types of clay, namely CloisiteNa and Cloisite30B, on the mechanical, thermal, and barrier properties of poly(butylene succinate) (PBS)/thermoplastic starch (TPS) blends have been studied. The properties of the blend nanocomposites were found to be dependent on nanoclay types and the blend ratio. For the nanocomposites containing high starch content (75 wt % TPS), the use of Cloisite30B led to an enhancement of the tensile modulus whereas the use of CloisiteNa provided superior thermal stability. The OTR and WVTR values of the PBS/TPS blend containing a high PBS ratio (75 wt %) also decreased significantly after adding the nanoclays. The results were ascribed to the different interactions between the two clays and the polymer blends as well as the different microstructures of the nanocomposites.

ACKNOWLEDGMENTS

The authors are sincerely grateful to the Higher Education Research Promotion and National Research University Project of Thailand, Office of the Higher Education Commission for providing a research grant to support this work (Project No.277).

REFERENCES

1. Available online at: ftp://ftp.jrc.es/pub/EURdoc/eur22103en.pdf (January, 2013).
2. Mani, R.; Bhattacharya, M. *Eur. Polym.* **2001**, *37*, 515.
3. Mani, R.; Bhattacharya, M. *Eur. Polym.* **1998**, *34*, 1467.
4. Bhattacharya, M.; Mani, R.; Tang, *J. Polym. Sci.* **1999**, *37*, 1693.
5. Park, H. W.; Lee, S. R.; Chowdhury, S. R.; Kang, T. K.; Kim, H. K.; Park, S. H.; Ha, C. S. *J. Appl. Polym. Sci.* **2002**, *86*, 2907.
6. Zenga, J. B.; Jiao, L.; Li, Y. D.; Srinivasanb, M.; Li, T.; Wang, Y. Z. *Carbohydr. Polym.* **2011**, *83*, 762.
7. Yu, L.; Dean, K.; Yuan, Q.; Chen, L.; Zhang, X. *J. Appl. Polym. Sci.* **2007**, *103*, 812.
8. Koh, H. C.; Park, J. S.; Jeong, M. A.; Hwang, H. Y.; Hong Y. T.; Ha S. Y.; Nam, S. Y. *Desalination* **2008**, *233*, 201.
9. Ray, S. S.; Bousmina, M. *Prog. Mater. Sci.* **2005**, *50*, 962.
10. Bocchini, S.; Battegazzore, D.; Frache, A. *Carbohydr. Polym.* **2010**, *82*, 802.
11. Nam, P. H.; Fujimori, A.; Masuko. T. *J. Appl. Polym. Sci.* **2004**, *93*, 2711.
12. Park, H. M.; Li, X.; Jin, C. Z.; Park, C. Y.; Cho W. J.; Ha C.S. *J. Macromol. Mater. Eng.* **2002**, *287*, 553.
13. Park, H. M.; Lee, W. K.; Park C. Y.; Cho, W. J.; Ha C. S. *J. Mater. Sci.* **2003**, *38*, 909.
14. Lee, S. R.; Park, H. M.; Lim, H.; Kang, T.; Li, X.; Cho, W. L.; Ha, C. S. *Polymer* **2002**, *43*, 2495.
15. Plackett, D. *J. Polym. Environ.* **2004**, *12*, 131.
16. Shin, B. Y.; Jo, G. S.; Kim, B. S.; Hong, K. S.; Jang, S. H.; Cho, B. H. *Appl. Chem.* **2006**, *10*,77.
17. Huneault, M.; Li, H. *Polymer* **2007**, *48*, 270.
18. Dean, K.; Yu, L.; Bateman, S.; Wu, D. Y. *J. Appl. Polym. Sci.* **2007**, *103*, 802.
19. Park, H. M.; Kim, G. H.; Ha, C. S. *Compos. Interfaces* **2007**, *14*, 427.
20. Available online at: http://ipruw.com/publications/2010/presentations/YiyoungChoi.pdf (January, 2013).
21. Thomassin, J. M.; Pagnoulle, C.; Caldarella, G.; Germain, A.; Jerome, A. R. *J. Membr. Sci.* **2006**, *270*, 50.
22. Duangkaew, P.; Wootthikanokkhan, J. *J. Appl. Polym. Sci.* **2008**, *109*, 452.
23. Boonsong, P.; Laohakunjit, N.; Kerdchoechuen, O.; Tusvil, P. *Inter. Food Research J.* **2009**, *16*, 97.
24. Available online at: http://www.nanoclay.com/selection_chart.asp (August, 2012).